Cathodoluminescence and growth of cassiterite in the composite lodes at South Crofty Mine, Cornwall, England

C. B. FARMER,* A. SEARL† AND C. HALLS*

* Mining Geology Research Group, Department of Geology, Royal School of Mines, Imperial College, London SW7 2AZ

† School of Earth Sciences, University of Birmingham, Edgbaston, Birmingham B15 2TT

Abstract

The cathodoluminescence (CL) of cassiterite (SnO_2) from the paragenetic sequence in the lodes at South Crofty Mines has been used in the interpretation of the processes which govern mineral deposition. Luminescence is controlled by the substitution of Ti, Fe and W for Sn in the cassiterite lattice. Ti and W behave as luminescence activators whereas Fe quenches luminescence. The observed colours and intensity of the luminescence are believed to result from the interplay between these effects. Successive generations of cassiterite formed during the separate stages of paragenetic evolution show different luminescence colours. These are believed to reflect changes in bulk composition of the fluid, which is indicated by the systematic variation in the composition of tourmaline in the associated gangue.

CL also reveals details of growth and deformation in individual crystals. Growth textures observed in CL are broad concentric growth banding, oscillatory zoning and sector zoning. Sector boundaries often show a zig-zag form which is indicative of competitive growth of adjacent crystal faces. Interpretation of CL textures is used to support the hypothesis that cassiterite growth took place under two main regimes. These are, firstly, conditions in which fluid pressure decreased abruptly when tectonic reactivation caused dilation of parts of the lode fracture system and secondly, conditions of sustained hydraulic pressure within fractured vein fill. In tectonically induced fractures the crystals are stubby, have non-equivalent growth faces and are commonly tetragonal bipyramidal forms in which sector zoning is invariably present. In hydraulic fractures crystals take a predominantly tetragonal prismatic form. Thus, it is believed that growth under these contrasting conditions leads to distinctive morphology and zoning in cassiterite, providing a basis for typomorphic characterisation.

KEYWORDS: cathodoluminescence, cassiterite, zoning, typomorphism, Cornwall.

Introduction

THE composite lodes at South Crofty Mine, Cornwall, U.K. contain multiple generations of cassiterite associated with tourmaline, chlorite, quartz and fluorite gangue. Descriptions of these veins, which are the classic form taken by tin mineralisation in the Camborne–Redruth mining district, have been given by Henwood (1843), Collins (1882), Flett (1903), MacAlister (1906), Dines (1956) and Hosking (1964). The complexity of the hydrothermal and tectonic processes responsible for the superimposed paragenetic stages in the lodes is evident in all these published descriptions. Two principal paragenetic stages associated with cassiterite mineralisation can be recognised. These are the earlier 'tourmaline stage', in which the gangue consists dominantly of tourmaline, followed by the 'chlorite stage', in which chlorite dominates over tourmaline. Structural and paragenetic studies (Farmer and Halls, in press) show that cassiterite is found in two main environments regardless of gangue mineralogy. Cassiterite mineralisation is hosted either (a) in discrete veins formed by structural reactivation of pre-existing fractures, or (b) in the matrix of hydraulic breccias.

Textural evidence, provided by the intergrowth of tourmaline and cassiterite, demonstrates that these two minerals are co-genetic. Interpretation

of hydrothermal chemistry therefore depends on a knowledge of the compositional variations in these two minerals and an understanding of the factors which govern these variations during paragenetic evolution. An independent constraint is provided by fluid inclusion microthermometry. Non-destructive electron beam analytical techniques (SEM–EPMA) provide a means of investigating compositional variations in tourmaline, however, levels of substitution in the cassiterite lattice lie at the limits of detection using wave-length dispersive (WD) analysis. Cathodoluminescence (CL) offers an alternative technique for studying, optically, the effects of cryptic elemental variations in the cassiterite lattice.

A considerable literature concerning the application of CL imagery to the interpretation of carbonate diagenesis, quartz growth and deformation and rare-earth activated luminescence of apatites and zircons now exists (see Marshall, 1988), however, there are only a few studies of cassiterite luminescence and there has been no systematic investigation of variations in cassiterite CL phenomena with respect to paragenetic sequence in a single deposit. Details of zoning and crystal growth are not easily observed using standard microscopic techniques, but CL images resolve these details and provide a basis for interpretation of compositional variations and the way in which these variations can be related to crystal growth.

In this study the chemical variation and zoning in cassiterite has been related to parallel variations in tourmaline chemistry and to thermometric measurements of fluid inclusions from the main stages of the paragenetic sequence preserved in the South Crofty lodes. These observations are used to interpret the mechanisms which are believed to govern cassiterite precipitation.

Instrumentation

Standard 30 μm polished thin sections were prepared from vein material collected at underground locations in South Crofty Mine. CL images were obtained using a Technosyn 8200 Mark II Cold Cathodoluminescence Stage mounted on a Nikon Labophot Microscope. This instrument was operated using a 20 kV accelerating voltage and 390 μA gun current. Under these conditions it was possible to obtain colour images on Kodak Ektar 1000 colour film at a magnification of 50× using 50 second exposures. CL spectra were generated using an S20 photomultiplier attached to a JEOL Superprobe in the Department of Materials, Imperial College. Point

analyses and element mapping were performed using a different JEOL 733 Superprobe in the WD mode with a 15 kv accelerating voltage, beam current of 40 μA and with the beam focused to a spot size of approximately 5 μm. Data collection was automated using programmable routines in LINK software. WD measurements were calibrated against both pure metal and oxide standards. EDS analyses of tourmaline were made using the same JEOL machine under operating conditions of 15 kv accelerating voltage and a beam current of 2 μA. Regular Co calibration and reference to known standards during analysis maintained maximum control on analytical quality. Thermometric measurements of fluid inclusions were made on a Linkam THM600 heating and freezing stage which was calibrated using synthetic fluid inclusions and chemical standards.

Cassiterite geochemistry

A number of accounts of the geochemistry of cassiterite exist in the scientific literature. These range from investigations of the chemical and physical factors governing the semiconductor properties of synthetic cassiterites to studies of the chemical variations found in natural cassiterites from a variety of metallogenic environments. Cassiterite has a tetragonal lattice structure similar to that of rutile, belonging to the p42/mnm space group. In a purely ionic model cassiterite would consist of close packed O^{2-} ions with Sn^{4+} ions occupying half the octahedral interstices. However, since the length of the Sn-O bonds in cassiterite have been measured at 20.5 nm and the sum of the ionic radii is 21.1 nm (Kohnke, 1962), it is evident that electron sharing between Sn and O occurs. This gives cassiterite the property of n-type semiconduction and permits a wide range of impurity elements to enter the structure diadochically.

Many diadochic substitutions in cassiterite have been recorded, both from the Cornubian orefield (e.g. Moore and Howie, 1979; Swinden, 1984; Hosking *et al.*, 1987) and other major tin provinces (e.g. Wolf and Espozo, 1972; Dulski, 1980; Izoret *et al.*, 1985). Following Goldschmidt's (1937) rules which assume a simple ionic structure, elements with ionic radii within ±12% of the Sn^{4+} radius (8.3 nm) could substitute diadochically. Schemes for the substitution of Sn^{4+} by transition metal impurities have been suggested by Möller *et al.* (1988), Izoret *et al.* (1985) and Ruck *et al.* (1989). These involve coupled substitutions of (Ta, Nb)-Fe and W-Fe pairs and direct substitution by Ti^{4+}.
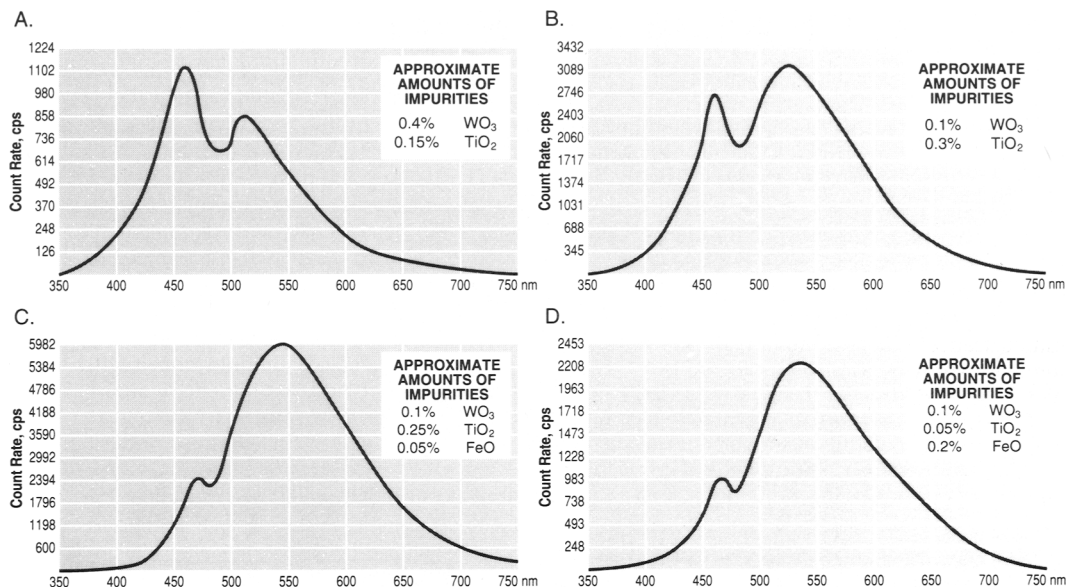
FIG. 1. Uncorrected spectra showing characteristics of cathodoluminescence corresponding to the different colours observed: (A) blue centre, (B) yellow rim (Plate 6a), (C) yellow band, (D) dark band (Plate 6b).

CL behaviour of cassiterite

By combining the results of WD analysis with CL spectra from mapped grains in samples from South Crofty it has been shown that blue luminescing zones (see Plate 5a) with distinctive spectral peaks at 460–465 nm (Fig. 1a) contain higher levels of W (Fig. 2a), whereas yellow luminescing zones (see Plate 5a) with spectral peaks at 520–550 nm (Fig. 1b,c) are enriched in Ti (Fig. 2b). Specific peaks are broadened due to interference by other spectral peaks of differing intensities (e.g. Fig. 1a–d). Where Fe is present together with Ti or W, quenching of luminescence causes a lowering of the intensity of the characteristic peaks although the spectra are otherwise similar (e.g. Plate 5b, Fig. 1c,d). These results are in accord with the earlier investigations of the CL behaviour of cassiterite made by Hall and Ribbe (1971) and by Rémond (1973).

On the basis of electron probe analyses of natural hydrothermal cassiterites, Hall and Ribbe (1971) concluded that Ti and W impurities are the chief activators responsible for cathodoluminescence. Characteristic emission bands were observed at peak wavelengths of about 565 nm and 440 nm respectively. Combinations of Fe, Ta and Nb substituting for Sn in cassiterite quench CL so the intensity of emitted light is decreased. Rémond (1973) has also suggested that Al and V can act as CL activators in cassiterite. However, spectral measurements made on synthetic films of

pure tin oxide by Bertrandt-Zytkowiak et al. (1988) showed that a peak occurs commonly at 560 nm, so intrinsic luminescence in cassiterite cannot be discounted.

A full spectral investigation using doped cassiterite samples has not been undertaken, so interpretations of CL effects are necessarily somewhat empirical. There are also other factors which could potentially activate luminescence in cassiterite and these have not been studied. They include vacancy-induced non-stoichiometry as in willemite (Bhalla and White, 1971), radiation damage as in diamonds (Mendelsohn et al., 1978) and dislocations as in authigenic quartz (Grant and White, 1978).

Zonal patterns in cassiterite

The techniques used to reveal subtleties of compositional zoning in minerals, such as the chemical etching of pyrite (e.g. Fleet et al., 1989) and the backscattered S.E.M. imagery of dolomite (e.g. Searl, 1989) do not serve to distinguish the delicate patterns of zoning in cassiterite. However, existing studies indicate that CL imagery is effective for this purpose.

Three types of zonal growth are observed and are classified as follows: —

Broad growth banding, in which the chemistry of the growing crystal responded progressive changes in the environment so that concentric

zones of variable width were formed, reaching a maximum of approximately 150 μm. Growth was continuous or interrupted leading to several characteristic patterns: —

(i) continuous growth produces a sequence of broad bands as shown in Plate 5a. In this example a blue luminescing core is surrounded firstly by a dull band in which luminescence is quenched and then finally by a broad band with a more yellow coloration.

(ii) continuous growth may also produce a cyclic pattern of luminescence as shown in Fig. 1c in which an alternating succession of broad blue and yellow luminescing bands are present.

(iii) interruptions in growth lead to unconformities in the pattern of concentric bands. Examples are shown in Plate 5d in which a nucleus of blue/dull luminescing cassiterite is overgrown by a bright yellow luminescing zone and in Plate 5e in which a yellow luminescing nucleus is overgrown by a blue/dull luminescing band.

Fine scale oscillatory zoning, in which an alternating sequence of thin bands (generally 15 μm or less) parallel to growth surfaces show different luminescence. For example, in Plate 5b repeated yellow and dark bands correspond with Ti-rich and Fe-rich compositional zones in the cassiterite crystal. Oscillatory zoning may occur together with broad growth banding and sector zoning (Plate 5b,e).

Sector zoning, in which parts of a crystal that formed under crystallographically different faces show variations in their luminescence colour and/or intensity. Sector zoning in the samples from South Crofty is of two distinct types. In the first type [101] sectors show blue luminescence and are W-activated. Examples of these blue sectors are found both in pyramidal section (Plate 5d) and
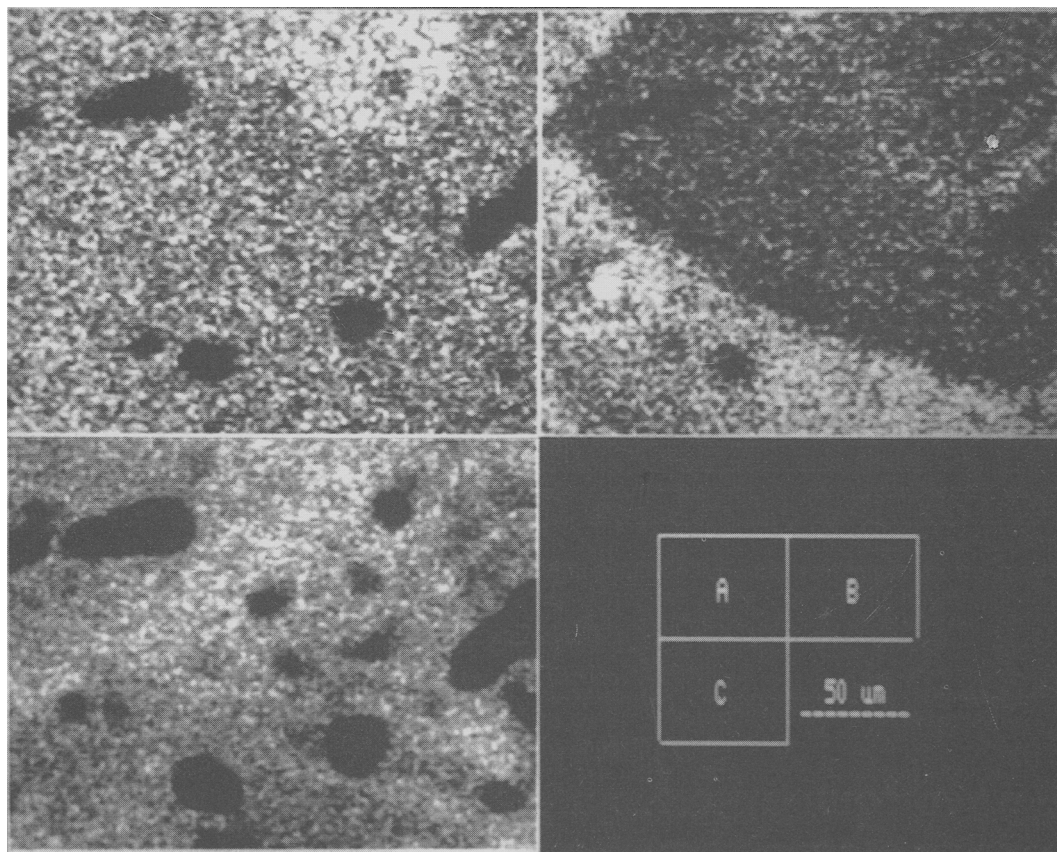

Fig. 2. Wave-length dispersive elemental maps showing the distribution of (A) W, (B) Ti and (C) Fe in the cassiterite crystal illustrated in Plate 6a. Brightness correlates with elemental concentration for each element but there is no correlation in brightness and absolute concentration between the different maps. In Fig. 1c the solid black areas are tourmaline inclusions which have been given a false colour.

basal section (Plate 5e). In the second type, [101] sectors show dull luminescence relative to adjacent sectors because of Fe-quenching (Plate 5a,b, Fig. 2c). W-activated sector zoning is more common early in the tourmaline stage of the paragenesis whereas, Fe-quenched sector zoning occurs late in the tourmaline stage and in the chlorite stage.

Discussion of types of zoning

By definition, compositional zoning in crystals is a non-ideal state of the lattice which arises because diffusion rates within the lattice are much less than the rates at which growth adds new material to the crystal surface. Compositional zones produced during crystal growth record progressive changes and/or local fluctuations in the physio-chemical environment from which the crystal grows. Hydrothermal experiments have demonstrated that diffusion of metal ions within the cassiterite lattice is negligible under hydrothermal conditions (Dusausoy, 1990, written communication). Systematic variations in the type of zoning in cassiterite should therefore reflect changes in fluid chemistry, pressure, temperature and fluid supply in the hydrothermal environment. There are three factors which control different types of compositional zoning: —

(i) progressive changes in the bulk composition of the fluid during particular stages in the sequence of mineralisation.

(ii) local fluctuations in the composition of the hydrothermal fluid near the surface of the growing crystals.

(iii) variations in the co-ordination of lattice sites available on different faces of the crystals growing in the hydrothermal medium.

(iv) growth mechanism.

Oscillatory zoning is generally explained in terms of kinetically controlled diffusion in the layer of solution immediately surrounding the growing crystal and is not directly related to changes in the bulk chemistry of the fluid, e.g. Haase et al. (1980), Allegre et al. (1981) and Loomis (1982). Mechanisms for the formation of oscillatory zoning in a variety of minerals have been reviewed and discussed by Searl (1989). In the case of cassiterites from South Crofty, the similarity in charge, electronegativity and size of Sn^{4+} ions and Ti^{4+} compared to Fe ions, may lead to preferential incorporation of Ti rather than Fe into the cassiterite from the solution boundary layer. This could account for the alternation of yellow luminescing and dull oscillatory zones which are revealed by CL (Plate 5b). In a dynamic hydrothermal regime, such as that responsible for

the vein system at South Crofty, it is unlikely that the oscillatory cycles will be exactly periodic. This lack of even periodicity in the spacing of oscillatory zones seen in CL images can be explained in terms of the perturbation of the solution boundary layer by turbulent flow through the fracture system (Huppert et al., 1987).

Broad growth banding is distinguished from oscillatory zoning by the greater width of individual bands and by the general lack of cyclicity. The progressive changes in composition which occurred during crystal growth are explained in terms of the evolving chemistry of the parent fluid. Abrupt changes in the composition of successive bands are likely to be the result of changes in fluid chemistry and/or dramatic changes in temperature or pressure which might cause periods of dissolution and would affect solid solution between tin and other elements. The structures and mineral textures observed in the South Crofty vein system demonstrate that hydrothermal and tectonic processes were interactive during mineralisation (Farmer and Halls, in press). There is reason to believe that pulses of fluid were throttled between segments of the fracture system so that episodes of rapid crystallisation in more or less closed domains were interrupted by movements which led to replenishment from adjacent, temporarily independent reservoirs which had evolved to slightly different compositions. Evidence for such a process is provided both by fluid inclusion chemistries and changes in the composition of the tourmaline gangue. Mixing of transitional fluids with waters from external sources can also be invoked during the later stages of paragenetic evolution.

Oscillatory zoning occurs in conjunction with some specific broad-scale growth bands (e.g. the predominantly yellow bands in Plate 5c). It is evident that conditions favouring the formation of oscillatory zoning were effective for only limited periods during growth, coinciding with certain ranges of solution chemistry, or particular physical conditions. Small fluid volume to crystal volume ratios within the fractures (probably in excess of $10^4:1$), permit temporal variations in solution chemistry.

Compositional sector zoning (e.g. Plate 5a,e) can only develop in minerals in which more than one crystal form are combined. The preservation of sector zoning depends on crystal growth and diffusion rates. A crystal will only show sector zoning if the rate of cation diffusion in the lattice is slower than the growth rate of that crystal (Nakamura, 1973). If many potential substituting ions are present in a solution, then competition for occupancy of the same lattice sites will occur.

Table 1.

Variation in Fe and Ti substitution in cassiterites from stages of the paragenesis discussed in the text.

Paragenetic Stage		Black T	Blue T	Quartz	Chlorite
Oxide		n=78	n=55	n=28	n=131
FeO	Maximum	0.188	0.342	0.173	0.431
	Mean	0.052	0.109	0.038	0.083
	Std.Dev.	0.047	0.087	0.040	0.081
TiO2	Maximum	0.378	0.229	0.580	0.396
	Mean	0.076	0.061	0.157	0.115
	Std.Dev	0.092	0.061	0.170	0.091

Aside from physical differences in size and electronegativity of the substituting ions, the main factor which will determine the order of preference is the non-equivalence of surface cation sites on different crystallographic forms. Incorporation of imperfectly sized impurity ions is governed by their co-ordination within partially completed growth faces or 'protosites' (Nakamura, 1973). Dowty (1976) explained sector zoning using the protosite concept and defined · the flexibility of each protosite on the basis of the number of completed bonds in the first coordination sphere. Considering octahedral sites, the capacity of a protosite to accept 'incorrect' atoms is inversely related to its fractional rating so sites with 5/6 partial co-ordination are less able to accept foreign atoms than 4/6 sites which are less able than 3/6 sites (Dowty, 1976; Reeder and Prosky, 1986). 1/6 and 2/6 sites would have weaker bonding so that impurity ions, although easily absorbed on the growing surface, would also be expelled readily from a new growth layer by surface diffusion (Dowty, 1976). Sites with 3/6 co-ordination are therefore considered most likely to retain impurity ions. In cassiterite the common forms are ranked in terms of their protosite co-ordination as follows: —

{110} form: 4.5/6 co-ordination
{001} form: 4/6 co-ordination
{111} form: 3.5/6 co-ordination
{101} form: 3/6 co-ordination
{100} form: 3/6 co-ordination

Thus, following Dowty (1976), the most likely sites for the preservation of substituting impurity ions in cassiterite occur on the {100} and {101} forms, as observed in the South Crofty cassiterites (Plate 5d,e).

The zig-zag boundaries between sectors, described as fir-tree zoning by Raven and Dickson (1989), can be explained in terms of differences in rates of growth in adjacent sectors (Sunagawa, 1984). The growth rate itself is controlled by a number of factors which include the roughness of the solid-liquid interface and the chemical potential difference between the solid and liquid (Sunagawa, 1984). Plate 5e shows that the dull luminescing sectors are wider, and have grown faster, where they coincide with dull luminescing oscillatory zones. This suggests that in cassiterite transient high Fe (possibly Ta and Nb) ion saturations in the boundary layer may influence inter-sectoral rates of growth.

Paragenetic relationships

Machel (1985), Reeder and Grams (1987) and others who have studied compositional zoning in carbonates have recommended caution when deducing changes in the bulk chemistry of fluids from zonal variations in crystal chemistry determined by point analytical techniques because chemical variation over a short range is often large. The cassiterites analysed in this study show a range of substitutions which give rise to complex variations in the composition of zoned crystals. For this reason it is only possible to make general deductions about the fluid chemistry during each stage of paragenetic evolution (Table 1). Because of this limitation further information about the T–X characteristics of the mineralising fluids is desirable.

At South Crofty, the two main stages of the cassiterite-bearing paragenesis have been characterised on the basis of variations in tourmaline composition supported by microthermometric studies of fluid inclusions. This information can be used in conjunction with the results of CL studies and cassiterite composition to provide better constraints on the interpretation of conditions under which mineralisation took place. Studies by Henry and Guidotti (1985) and Jolliff et al. (1986) show that tourmaline compositions reflect the bulk chemistry of the systems in which

they formed and provide valuable independent evidence of variations in fluid composition during paragenetic evolution. The Ti and Fe concentrations in tourmaline are particularly useful because they can be correlated with CL response in the associated cassiterite. The levels of W in tourmaline have not been determined but its presence as an impurity in cassiterite from all the paragenetic stages suggests it is a persistent component of the mineralising fluid.

The first main stage of the tin-bearing paragenesis, the tourmaline stage, contains a gangue of tourmaline with subordinate quartz. The first cycle of the tourmaline stage is characterised by unzoned, compositionally homogeneous tourmaline grains. In hand specimen these tourmalines show a progressive change in colour from black at the beginning of the cycle to blue at the end of the cycle. Both varieties are penetratively intergrown with cassiterite. Tourmaline compositions evolve towards the schorlitic (Fe-rich) end-member in each cycle of mineralisation (Fig. 3). A corresponding decrease in Ti content is also observed, which is a reflection of the progressive reduction of Ti/Fe ratios in the fluid (Fig. 4) Concurrently, the CL response of cassiterite changes from the yellow and blue colours activated by Ti and W to increasingly dull brown and blue Fe-quenched luminescence (Plate 5e,f). A second cycle of vein tourmaline-cassiterite mineralisation has also been identified. In this case, blue–green coloured
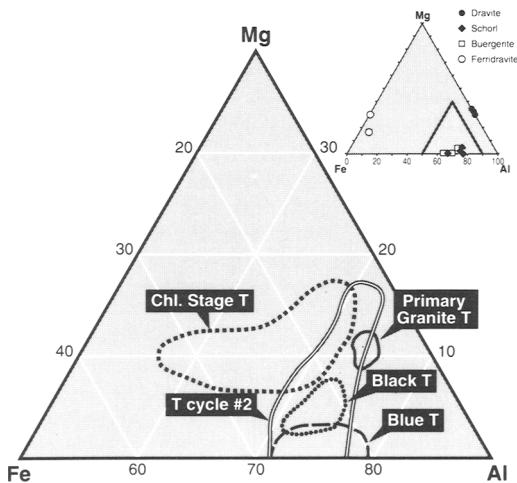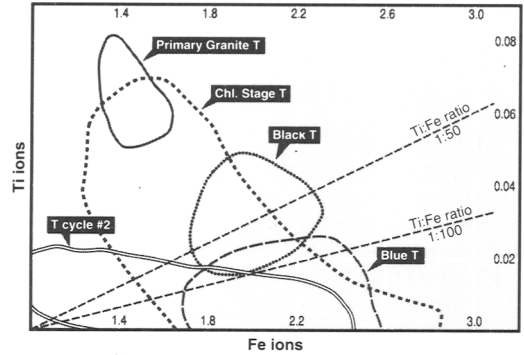

FIG. 4. Iron vs. titanium plot for tourmalines from specific paragenetic stages (data set consists of approx. 570 probe analyses).

tourmalines have more dravitic (Mg-rich) compositions (tourmaline cycle #2, Fig. 3) and are less Ti-rich. However, high Ti/Fe ratios are found in tourmalines at the start of this second cycle (Fig. 4) and give rise to yellow luminescence in cassiterite. These can be found as overgrowths on earlier dull-blue luminescing cassiterites (Plate 5d). In hydraulic fractures containing a dominant gangue of quartz with only minor tourmaline (which is the only Fe-bearing mineral at this stage of the paragenesis), cassiterite luminescence is most intense because of the absence of Fe-quenching (Plate 5c).

In the chlorite stage which is the second major stage of the cassiterite-bearing paragenesis at South Crofty, tourmaline is subordinate to Fe-chlorite in the gangue, however this tourmaline can be compared to those of earlier paragenetic stages. Individual tourmaline crystals show distinct broad-scale growth banding with compositions tending towards ferridravite with low Ti/Fe ratios, and dravite with high Ti/Fe ratios (Figs. 3 and 4). Cassiterite of the chlorite stage shows distinctive bright yellow and dark oscillatory zones combined with broad growth banding (Plate 5b).

Microthermometric analysis of fluid inclusions in cassiterite and associated gangue minerals, particularly quartz, has provided homogenisation (Th) and ice melting (Tm_{ice}) temperatures of the mineralising fluids (Fig. 5). The summary diagram provides a framework within which the measurements of inclusions in cassiterite can be interpreted. Inclusions in cassiterite of both the tourmaline and chlorite stages which are not in obvious microfractures and are probably of primary origin have relatively high homogenisation temperatures (Table 2). Within the tourmaline stage, the cassiterites intergrown with black

FIG. 3. Magnesium–iron–aluminium ternary diagram of tourmaline compositions from specific paragenetic stages determined by EPMA (data set consists of approx. 570 probe analyses). Inset shows typical positions of end-member tourmaline species (after Deer et al., 1986).
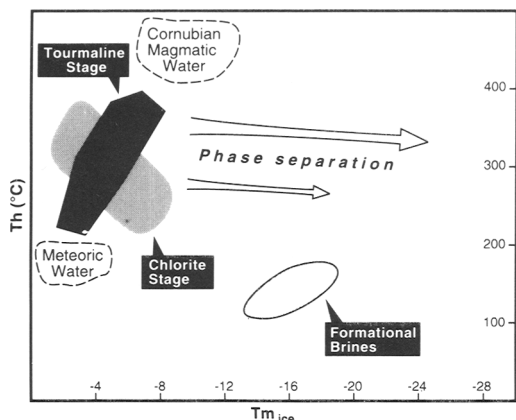
FIG. 5. Summary diagram of microthermometric data obtained from fluid inclusions in gangue minerals from each broad paragenetic stage at South Crofty Mine (data set consists of over 600 paired measurements).

tourmaline have slightly higher Th than those intergrown with later blue tourmaline. Within the chlorite stage the range of homogenisation temperatures is noticeably wider. It is assumed that pressure corrections would not significantly affect the relative values of the sets of Th data, so it is inferred that cassiterite deposition took place during the hottest (earliest?) part of each paragenetic sub-stage. In the tourmaline sub-stages of the paragenesis, Th values cover only a narrow range which, considering temperature dependent solid solution mechanisms alone, could not account for the extent of elemental substitution observed in these cassiterites. The large range in Tm_{ice} (i.e. salinity) is a consequence of the trapping of fluids with high but variable salinity. These are believed to be residual fluids formed during the separation of a H_2O-rich vapour phase, and because these inclusions co-exist with the vapour-rich inclusions and have similar homogenisation temperatures, they are assumed to be co-genetic (e.g. Ramboz *et al.*, 1982). The separation is believed to have been caused by reduc-

tion of pressure during successive structurally regulated dilations of the lode system.

Cassiterites from the tourmaline stage of the paragenesis are believed to have been crystallized from fluid of magmatic departure. Tourmaline compositions show a magmatic fractionation trend with progressively lower Mg/Fe and Ti/Fe ratios (e.g. Nieva, 1974, and Power, 1968). The trend of decreasing salinity and temperature revealed in the fluid inclusions from the tourmaline stage (Fig. 5) can also be explained as a result of the entrapment of fluids generated progressively during the crystallisation of a hydrous magma (Bodnar and Cline, 1990) without invoking mixing with cooler meteoric waters (e.g. Jackson *et al.*, 1989). However, in the chlorite stage of the paragenesis, tourmaline compositions can be interpreted in terms of mixing between a magmatic fluid and more oxidizing exo-granitic fluids (e.g. formational brines and/or meteoric waters, Fig. 5) within spaces created by reactivation of the fractures hosting the earlier tourmaline stage of mineralisation.

Typomorphism of cassiterite and depositional environments

The dominant forms contributing to crystal shape can be identified using CL imagery, and morphology appears to be systematically linked to conditions of deposition at various stages of paragenetic evolution. This variation forms a basis for the definition of typomorphic facies.

In the tourmaline stage, cathodoluminescence shows that stubby cassiterite crystals, with dimensions along the crystallographic *c*-axis similar to those in the *a*- and *b*-axis directions, are dominated by the tetragonal bipyramids {111} and {101} in combination with the minor pinacoid (001) and prism faces (110) and (100). In cassiterites of this stage, sectors of the {101} form are commonly W-enriched and show blue luminescence. In cassiterites associated with predominantly quartz gangue, which are typically formed

Table 2.

Microthermometric data for fluid inclusions in cassiterites from the paragenetic stages at South Crofty Mine. All temperatures have been corrected against calibration curves and are given in degrees Celsius.

Paragenetic Stage		Temperature of Homogenization (Th)	Temperature of Ice Melt (Tm_{ice})
Tourmaline	Black	360 to 375	−6 to −12
	Blue	280 to 340	−4 to −26
	Quartz	300 to 350	−5 to −12
Chlorite		260 to 340	−3 to −10

in hydraulic breccias, different morphologies are observed. Few prism faces are developed, commonly (110) faces only are present, giving the crystals trapezoid forms in thin section (Plate 5c). Protracted histories of growth and dissolution are revealed by unconformable overgrowths within each crystal and occasionally quartz crystals nucleate on the growth surfaces of cassiterite (Plate 5c). The morphology of cassiterites from the chlorite stage of the paragenesis is complex (Plate 5b) with a combination of bipyramid and prism faces, complicated by twinning. Sector zoning is also common, with high levels of Fe impurities in [101] sectors.

In his detailed study of the crystal forms of cassiterite from the Kalima region in Zaire, Varlamoff (1949) recognised a systematic variation in the dominant crystal forms found at different depths in and around isolated granite plutons. He concluded that these variations were independent both of the type of host rock and the mode of emplacement, whether in open fractures or by replacement. He therefore postulated that these were typomorphic variations related to systematic changes in temperature and pressure around and within the plutonic bodies. Varlamoff observed that the outer zone of cassiterites tended to show more prismatic habits dominated by the forms $\{110\}$ and $\{100\}$ whereas those from the interior zones were dominated by the forms $\{111\}$ and $\{101\}$. This perception of typomorphic zoning takes no account of the dynamic factors operating in the environment of deposition.

Within the tourmaline stage, textural evidence, such as the even, fine-grained, penetrative intergrowth of tourmaline needles with the quartz gangue (Plate 5e) suggests that nucleation and growth of quartz and tourmaline took place simultaneously and rapidly in response to reductions in confining pressure caused by fault reactivation. It is evident from textural studies of orthomagmatic tourmaline breccias that borosilicate fluids respond to abrupt falls in pressure by crystallising masses of microcrystalline tourmaline (e.g. Allman-Ward et al., 1982). It is believed that in the South Crofty lodes, the early formation of discrete fractures filled by microcrystalline tourmaline gangue was also chiefly pressure-controlled. Rapid fluid pressure reduction which triggers nucleation of tourmaline and separation of a H_2O-rich vapour phase within the fluid, also leads to the co-precipitation of cassiterite. The small size and even dissemination of cassiterite crystals is consistent with high nucleation rates and therefore high degrees of supersaturation, Plate 5a (e.g. Mullin, 1972). In samples containing larger but still evenly spaced and equally sized crystals, relatively fewer nuclei were formed, indicating a lower degree of supersaturation. The precipitation of tourmaline and cassiterite together with the separation of a vapour phase triggered by the initial pressure drop depletes the fluid in tin and borosilicate components but leaves a pressurised residue. Further fracturing and hydraulic brecciation could be expected to occur leading to the formation of veins with quartz as the main gangue mineral. At this stage pressures could be sustained with only slight fluctuations as the fractures propagate. The fluids, now depleted in tin species, could be expected to reach saturation more slowly as the fluid cooled. The elongated morphology of the crystals and the parasitic nucleation of quartz on their growing surfaces may indicate that they grew in vapour (Thiel and Helbig, 1976) or within a gel.

The growth of cassiterites in the chlorite stage is inferred to have been governed by mixing of hot, magmatically-derived fluids with cooler exogranitic fluids. The chief factor governing cassiterite precipitation, both in the chlorite stage and in the quartz-filled hydraulic fractures, was evidently reduction in fluid temperatures (e.g. Eadington, 1988). The factors controlling the difference in morphology between cassiterites from the chlorite stage and cassiterites from quartz-filled hydraulic fractures could be:

(a) systematic differences in fluid temperature and pressure which, together, would control levels of supersaturation and thus the growth mechanism operating on non-equivalent faces. Growth rates on non-equivalent faces could be expected to be different because transitions between different types of growth mechanism occur at different levels of supersaturation for non-equivalent faces (Sunagawa, 1977).

(b) systematic differences in fluid composition, for example in the concentration of Fe, which may poison particular growth surfaces, or

(c) heterogeneity in the mixing fluids of the chlorite stage, which could cause irregularities in crystal growth.

In attempting to explain morphological variations in cassiterite from the different paragenetic stages which compose the lode system at South Crofty Mine it is necessary to take into account not only the conditions of temperature and pressure under which mineralisation occurred, but also the composition of the fluids, the rate at which conditions were changing and the mechanisms which could be responsible for those changes. The combination of evidence from CL imagery, fluid inclusion studies and the textural and paragenetic relations of cassiterite from South Crofty Mine shows that the relationship

between fracturing and fluid behaviour during the stages of the paragenetic evolution were different. These differences explain the patterns of minor elements substituting for Sn in the cassiterite lattice and also provide a basis for the interpretation of typomorphic variation in terms of dynamic tectonic and fluid processes.

Conclusions

Systematic variations in zoning and morphology of cassiterite from South Crofty have been studied using cathodoluminescence imagery. The spectra produced during electron bombardment can be related to specific CL activating or quenching impurities substituting in the cassiterite lattice. The analyses presented are consistent with Ti activation of yellow luminescence, W activation of blue luminescence and the quenching of luminescence by Fe impurities, as reported in previous studies. The CL responses of cassiterite from different stages of the paragenetic sequence correlate with the Ti and Fe contents of co-existing tourmalines. W is evidently present in the mineralising fluids throughout the history of evolution of the South Crofty lodes.

Fe substitution in cassiterites increases progressively throughout the tourmaline stage of the paragenesis. The highest levels are associated with Fe-enriched blue tourmaline and the lowest range of homogenisation temperatures. This demonstrates that the level of substitution of iron in cassiterite is directly related to the concentration of iron in the mineralising solutions. On the basis of trends in tourmaline composition, the corresponding change in Ti content of cassiterites in the tourmaline stage of the paragenesis probably also reflects changes in solution chemistry. This is likely to be the general case for most substitutions of transition metal elements in the cassiterite lattice because their ionic radii and electron field strengths are similar to that of the Sn^{4+} ion.

Episodic supply of fluids during the stages of mineralisation plays an important role in determining patterns of zonation during crystal growth. The textures of cassiterite revealed by CL can be attributed to two factors: (*a*) variations in the composition of the mineralising fluid; (*b*) variations in the tectono–hydrothermal conditions, i.e. pressure and/or temperature, governing cassiterite deposition.

In turn these factors determine the dominant form in which the cassiterite crystals grow. From these considerations it is clear that factors other than temperature and pressure must be taken into account when seeking an explanation for typomorphic variations of mineral species in hydrothermal systems.

References

Allegre, C. J., Provost, A., and Jaupart, C. (1981) Oscillatory zoning. A pathological case of crystal growth. *Nature*, **294**, 223–8.

Allman-Ward, P., Halls, C., Rankin, A. H., and Bristow, C. M. (1982) An intrusive hydrothermal breccia body at Wheal Remfry in the western part of the St. Austell granite pluton, Cornwall. In *Metallization associated with acid magmatism* (Evans, A. M., ed.), Wiley, 1–28.

Bertrandt-Zytkowiak, M., Chimczak, E., and Gordon, W. S. (1988) Cathodoluminescence spectra of thin tin oxide films. *Acta Phys. Polonica*, **A73**, 535–41.

Bhalla, R. J. R. S. B. and White, E. W. (1971) Intrinsic cathodoluminescence emission from willemite single crystals. *J. Lumin.*, **4**, 194–200.

Bodnar, R. J. and Cline, J. S. (1990) Microthermometric and phase behaviour of magmatic-hydrothermal fluid inclusions: An analysis based on PVTX data for the system albite–H_2O–NaCl. *PACROFI III Abstracts*, Toronto, p. 17.

Collins, J. H. (1882) On some Cornish tin stones and tin capels (second part). *Mineral. Mag.*, **4**, 103–16.

Deer, W. A., Howie, R. A., and Zussman, J. (1986) *Rock-forming Minerals*, Volume 1B: *Disilicates and Ring Silicates* (2nd ed.) Longman Scientific & Technical, Harlow, U.K.

Dines, H. G. (1956) The metalliferous mining region of southwest England. *Mem. Geol. Survey*, U.K., H.M.S.O., London, 795 p.

Dowty, E. (1976) Crystal structure and crystal growth: II. Sector zoning in minerals. *Am. Mineral.*, **61**, 460–9.

Dulski, P. (1980) Spurenanalyse als Hilfsmittel bei der geochemischen Untersuchung der Genese bolivian-

scher Zinnerzlagerstätten. *Verlag von Dietrich Reimer*, Berlin, 79pp.

Eadington, P. J. (1988) The solubility of cassiterite in hydrothermal solutions in relation to some lithological and mineral associations of tin ores. In *Recent advances in the geology of granite-related mineral deposits* (Taylor, R. P. and Strong, D. F., eds.), 25–32.

Farmer, C. B. and Halls, C. (in press) Controls on cassiterite mineralisation at South Crofty Mine, Cornwall, United Kingdom. *Proceedings of the 8th IAGOD Symposium Ottawa 1990.*

Fleet, M. E., MacLean, P. J., and Barbier, J. (1989) Oscillatory-zoned As-bearing pyrite from strata-bound and stratiform gold deposits: An indicator of ore fluid evolution. *Econ. Geol. Monograph 6*, 356–62.

Flett, J. S. (1903) Note on some brecciated stanniferous veinstones from Cornwall. *Sum. Prog. Geol. Serv. for 1903*, 150–62.

Goldschmidt, V. M. (1937) The principles of distribution of chemical elements in minerals and rocks. *J. Chem. Soc.*, 655–73.

Grant, P. R. and White, S. H. (1978) Cathodoluminescence and microstructure of quartz overgrowths. In *Scanning Electron Microscopy, 1978/1* (Johari, O., ed.), 789–94.

Hall, M. R. and Ribbe, P. H. (1971) An electron microprobe study of luminescence centres in cassiterite. *Am. Mineral.*, **56**, 31–46.

Haase, C. S., Chadham, J., Feinn, D., and Ortaleva, P. (1980) Oscillatory zoning in plagioclase feldspar. *Science*, **209**, 272–4.

Henwood, W. J. (1843) On the metalliferous deposits of Cornwall and Devon. *Trans. Roy. Geol. Soc. Cornwall*, **5**, 1–386.

Henry, D. J. and Guidotti, C. V. (1985) Tourmaline as a petrogenetic indicator mineral: an example from the staurolite-graded metapelites of NW Maine. *Am. Mineral.*, **70**, 1–15.

Hosking, K. F. G. (1964) Permo-carboniferous and later primary mineralisation of Cornwall and South-west Devon. In *Present views of some aspects of the geology of Cornwall and Devon* (Hosking, K. F. G., Shrimpton, G. J., eds.), 150th Anniversary Volume, Royal Geological Society of Cornwall, 201–45.

——Stanley, C. J., and Camm, G. S. (1987) The occurrence, nature and genesis of wood tin in South-west England. *Trans. Royal Geol. Soc. Cornwall*, **21**, 153–212.

Huppert, H. E., Sparks, R., Stephen, J., Wilson, J. R., Hallworth, M. A., and Leith, A. M. (1987) Laboratory experiments with experiments with aqueous solutions modelling magma chamber processes; II, Cooling and crystallisation along included planes. In *Origins of igneous layering* (Parsons, I., ed.), *NATO Advanced Study Institutes Series, Series C: Mathematical and Physical Sciences*, **196**, 539–68.

Izoret, L., Marnier, G., and Dusausoy, Y. (1985) Charactérisation cristallochimique de la cassitérite des gisements d'étain et de tungstène de Galice, Espagne. *Can. Mineral.*, **23**, 221–31.

Jackson, N. J., Willis-Richards, J., Manning, D. A. C., and Sams, M. (1989) Evolution of the Cornubian orefield, S.W. England. Part II: Mineral deposits and ore-forming processes: *Econ. Geol.*, **84/5**, 1101–33.

Jolliff, B. L., Papike, J. J., Shearer, C. K., and Laul, J. C. (1986) Tourmaline as a recorder of pegmatite evolution: Bob Ingersoll pegmatite, Black Hills, South Dakota. *Am. Mineral.*, **71**, 472–500.

Kohnke, E. E. (1962) Electrical and optical properties of natural stannic oxide crystals. *J. Phys. Chem. Solids*, **23**, 1557–62.

Loomis, T. P. (1982) Numerical simulation of crystallisation processes of plagioclase in complex melts: the origin of major and oscillatory zoning in plagioclase. *Contrib. Min. Petrol.*, **81**, 219–29.

MacAlister, D. A. (1906), Pt. II, Mining. In: The geology of Falmouth and Truro and of the mining district of Cambourne and Redruth (Sheet 352). *Mem. Geol. Surv. Eng. and Wales*, 335pp.

Machel, H. G. (1985) Cathodoluminescence in calcite and dolomite and its chemical interpretation. *Geoscience Canada*, **12**, 139–47.

Marshall, D. J. (1988) *Cathodoluminescence of geological materials*, Unwin-Hyman, Boston, 146pp.

Mendelssohn, M. J., Milledge, H. J., Vance, E. R., Nave, E., and Woods, P. A. (1978) Internal radioactive haloes in diamonds. In *Industrial Diamond Review*, 31–6, London.

Möller, P., Dulski, P., Szack, W., Malow, G., and Riedel, E. (1988) Substitution of tin in cassiterite by tantalum, niobium, tungsten, iron and manganese. *Geochim. Cosmochim. Acta*, **52**, 1497–503.

Moore, F. and Howie, R. A. (1979) Geochemistry of some Cornubian cassiterites. *Mineral. Deposita*, **14**, 103–7.

Mullin, J. W. (1972) *Crystallisation* (Second Edition), Butterworths, London, 480pp.

Nakamura, Y. (1973) Origin of sector zoning in igneous clinopyroxenes. *Am. Mineral.*, **58**, 986–90.

Neiva, A. M. R. (1974) Geochemistry of tourmaline (schorlite) from granites, aplites and pegmatites from northern Portugal. *Geochim. Cosmochim. Acta*, **38**, 1307–17.

Power, G. M. (1968) Chemical variation in tourmaline from South-west England. *Mineral. Mag.*, **36**, 1078–89.

Ramboz, C., Pichavant, M., and Weisbrod, A. (1982) Fluid immiscibility in natural processes: use and misuse of fluid inclusion data. *Chem. Geol.*, **37**, 1–48.

Raven, M. J. and Dickson, J. A. D. (1989) Fir-tree zoning: an indicator of pulsed crystallisation in calcite cement crystals. *Sediment. Geol.*, **65**, 249–59.

Reeder, R. J. and Grams, C. (1987) Sector zoning in calcite cement crystals: Implications for trace element distribution in carbonates. *Geochim. Cosmochim. Acta*, **51**, 187–94.

——and Prosky, J. L. (1986) Compositional sector zoning in dolomite. *J. Sed. Pet.*, **56**, 237–47.

Rémond, G. (1973) Exemples d'identification et de localisation des éléments en traces dans les minéraux luminescents (cassitérites), à l'aide de l'analyseur ionique. *Bull. Soc. franç. Minéral. Crist.*, **96**, 183–98.

Ruck, R., Dusausoy, Y., Nguyen Trung, C., Gaite, J-M., and Murciego, A. (1989) Powder EPR study of

natural cassiterites and synthetic SnO_2 doped with Fe, Ti, and Na and Nb. *Eur. J. Mineral.*, **1**, 343–52.

Searl, A. (1989) Saddle dolomite: a new view of its nature and origin. *Mineral. Mag.*, **53**, 547–55.

Sunagawa, I. (1977) Natural crystallisation. *J. Crystal Growth*, **42**, 214–23.

—— (1984) Growth of crystals in nature. In *Materials Science of the Earth's Interior* (Sunagawa, I., ed.), Tokyo, Terra Scientifica, 63–105.

Swinden, T. R. (1984) *An investigation of the variations in optical properties and chemical composition of cassiterite in Cornish tin deposits.* Unpubl. Ph.D. thesis, Camborne School of Mines.

Thiel, B. and Helbig, R. (1976) Growth of SnO_2 single crystals by vapour phase reaction method. *J. Crystal Growth*, **32**, 259–64.

Varlamoff, N. (1949) Relations entre les faciés des cristaux de cassitérite de la region Kalima (Congo Belge) et la geologie de leurs gisements. *Ann. Soc. Geol. Belg.*, **72**, 289–316.

Wolf, D. and Espozo, E. (1972) Zur Geochemie bolivianischer Kassiterite. *Z. Angewandte Geol.*, **18**, 459–68.
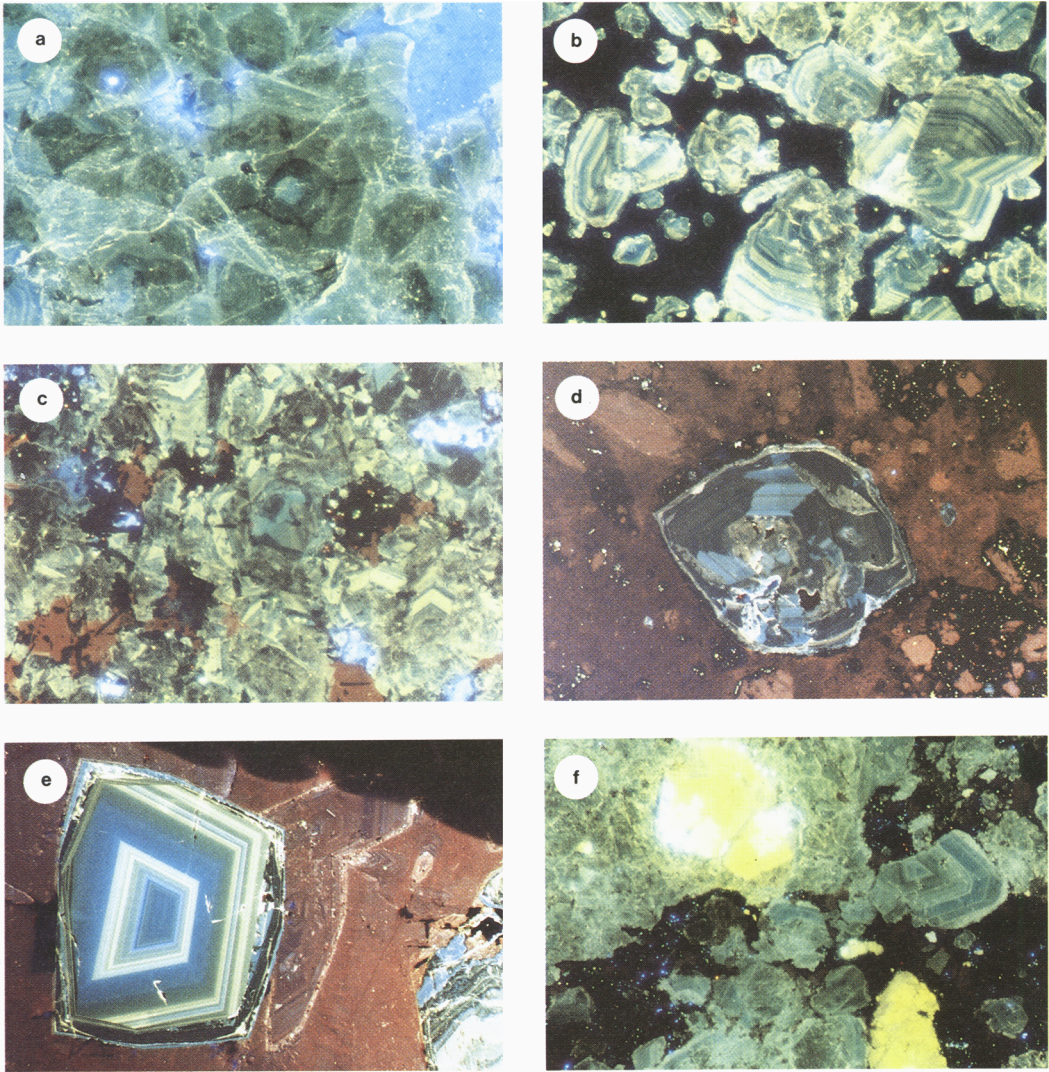
PLATE 5. (*a*) Cathodoluminesence (CL) image of a cassiterite crystal showing a blue luminescing core, quenched cross-shaped sectors and yellow luminescing rim. The bright blue luminescing areas are fluorite (the long dimension of image is 0.65 mm). (*b*) CL image of cassiterite showing fine scale oscillatory zoning within yellow and dark banding. Duller luminescing discordant zones are largely an artifact of light reflection within the crystal, except in the oval-shaped crystal to the left of the figure which exhibits Fe-quenched sector zoning. The non-luminescing areas consist of chlorite (the long dimension of image is 0.65 mm). (*c*) CL image of cassiterite crystal showing a blue/dull luminescing sector-zoned core and yellow luminescing overgrowth. The gangue consists of non-luminescing tourmaline, red-luminescing quartz and bright luminescing specks of fluorite (the long dimension of image is 0.65 mm). (*d*) CL image of cassiterite with a yellow luminescing core, blue/dull luminescing sector zoning, dissolution and an overgrowth in which the pattern of luminescence is repeated. The pink luminescing mineral is quartz, and where intergrown with non-luminescing tourmaline it shows a purple colour (the long dimension of image is 2.6 mm). (*e*) CL image of cassiterite showing broad blue and yellow growth bands with superimposed fine scale oscillatory zoning. Discordant zones define a dissolution surface with cassiterite overgrowth. Euhedral, purple luminescing quartz grains nucleate on the overgrowth surface (the long dimension of the image is 2.6 mm). (*f*) CL image of cassiterites with bright yellow luminescing apatites. The cassiterites show yellow and blue luminescing growth bands (the long dimension of image is 1.3 mm).